JOURNAL OF PROPULSION AND POWER
Vol. 19, No. 3, May–June 2003

Study of Interspacecraft Coulomb Forces and Implications for Formation Flying

Lyon B. King,* Gordon G. Parker,† Satwik Deshmukh,‡ and Jer-Hong Chong‡
Michigan Technological University, Houghton, Michigan 49931

In the course of exploiting spacecraft formations for use in separated interferometry (or other missions), it is possible that the separation distance between vehicles will be on the order of 10 m. The effects of spacecraft charging on the dynamics of very closely spaced formations are investigated. For certain high-Earth orbits, the ambient plasma conditions will conspire to produce significant spacecraft charging in an environment with a plasma Debye length of more than 100 m. For such conditions, it is shown that the potential exists to develop disruptive interspacecraft Coulomb forces and torques, with magnitude comparable to candidate formation-keeping thrusters over distances of tens of meters. Because of the unexpectedly large interaction forces, the concept of purposely charging spacecraft to affect formation-keeping Coulomb forces is also explored. Analytic methods are developed that show the existence of static equilibrium formations in Earth orbit using only inter-vehicle coulomb forces for one-, two-, and three-dimensional formations. Such Coulomb formations would be free of the risk of plume contamination due to thrusters firing in close proximity. Figures of merit for the proposed Coulomb control system are calculated in a manner analogous to traditional propulsion systems, and it is shown that required forces can be created with milliwatts of power, can be controlled on a millisecond timescale, and imply specific impulses that can be as high as 10^{13} seconds.

Nomenclature

C = capacitance, F
d = spacecraft separation, m
$d_{i,j}$ = separation distance between the ith and the jth particles, m
E_i = electric field at a point i on spacecraft, V/m
F_{AB} = net (coulomb) force on spacecraft A resulting from the n_B charges on spacecraft B, N
$F_{i,j}$ = coulomb force between the ith and the jth particles, N
g_0 = gravitational constant, m/s^2
I_{eA} = emission current of spacecraft A, A
J_p = absorbed plasma current density, A/m^2
k = Boltzmann constant, J/K
L = distance from the combiner to collector, m
m_i = spacecraft mass, kg
$\dot{m}$ = ejected mass flow rate, kg/s
n_B = number of elements (charges) on spacecraft B
n_e = electron density, m^{-3}
n_i = ion density, m^{-3}
P = power, W
$\boldsymbol{p}_i$ = position vector of the ith vehicle, m
Q_i = charge on the ith vehicle, C
q_i = charge in the ith particle, C
r_i = radius of the ith spacecraft, m
$\boldsymbol{r}_{ij}$ = vector from point i to point j, m
T_e = temperature of electrons, K
T_{ion} = temperature of ions, K
t = time, s
u_e = exhaust velocity at which the mass is emitted, m/s
V_i = vehicle surface potential, V
v_i = potential of the ith element on the spacecraft surface, V
ε_0 = electrical permittivity of the vacuum, C^{2}N^{-1}m^{-2}
κ_c = Coulomb's constant, N m^2/C^2
λ_d = plasma Debye length, m
Ω = orbital angular velocity, rad/s

Received 16 September 2002; revision received 14 February 2003; accepted for publication 17 February 2003.

*Assistant Professor, Mechanical Engineering—Engineering Mechanics; lbking@mtu.edu.
†Associate Professor, Mechanical Engineering—Engineering Mechanics, 1400 Townsend Drive. Member AIAA.
‡Graduate Research Assistant, Mechanical Engineering—Engineering Mechanics.

I. Introduction

SWARMS of microsatellites are envisioned as an alternative to traditional large spacecraft. Such swarms, acting collectively as virtual satellites, will benefit from the use of cluster orbits where the satellites fly in a close formation.[1] The formation concept, first explored in the 1980s to allow multiple geostationary satellites to share a common orbital slot,[2,3] has recently entered the era of application with many missions slated for flight in the near future. The promised payoff of formation flying has recently inspired a large amount of research in an attempt to overcome the rich technical problems. A variety of papers can be found on the subject,[4–6] as well as a recent textbook on micropropulsion,[7] and numerous other sources.[8–12]

Relative position control of multiple spacecraft is an enabling technology for missions seeking to exploit satellite formations. Of the many technologies that must be brought to maturity to realize routine formation flying, perhaps the most crucial is the spacecraft propulsion system. The most challenging propulsion system demands will be made in close formations, where intervehicle spacing may be as small as 5 or 10 m. Apart from the obvious danger of collision, exhaust plume contamination of sensitive instruments is a legitimate concern for spacecraft in a formation. In close proximity, the propellant emitted by such devices as vaporized Teflon® (micro-PPTs), ionized cesium (FEEP), or colloid thrusters (liquid glycerol droplets doped with NaI) may impinge on neighboring vehicles with the potential to damage payloads. To worsen the problem, orbital mechanics for many clusters of interest mandate continuous thruster firings pointed directly toward other vehicles in the formation.

Work reported in this paper represents what the authors believe is a new mode of propulsive interaction between spacecraft in close formation. The interaction arises from Coulomb forces between vehicles in a swarm of electrically charged spacecraft. Forces can be produced as a result of natural charging due to space plasma interaction. In the case of natural charging, the Coulomb forces represent perturbations on vehicles in the formation that onboard thrusters must counteract. It will be shown in the following sections that, in high orbits such as geostationary-Earth orbit (GEO), natural charging

is capable of producing forces and torques with magnitudes comparable to those of microthrusters over separation length scales of tens of meters.

In addition to an analysis of parasitic Coulomb forces from space plasma interaction, this paper reports on an exploratory study to examine the feasibility of using Coulomb forces to maintain rigid satellite formations in high Earth orbit. In the Coulomb control scenario, onboard power would be used to charge vehicles in a swarm actively, to affect formation-keeping forces and possibly act as an emergency collision avoidance system. The use of Coulomb forces would provide nearly propellantless formation control with little or no risk of exhaust plume contamination of neighboring vehicles. Analytic and numeric calculations show that the dynamic equations permit rigid Coulomb formations in orbit and that these formations are controllable in three dimensions. It is also shown that the amount of onboard power required to affect charge control is negligible and that continuous thrust variation is possible over rapid time scales.

II. Coulomb Perturbations

A. GEO Plasma Environment

The Coulomb force between two point charges in the presence of plasma is represented by the typical inverse square relationship modified by an exponential term to account for the Debye shielding

$$F_{1,2} = (1/4\pi\varepsilon_0)\left(q_1 q_2 \Big/ d_{1,2}^2\right)\exp(-d_{1,2}/\lambda_d) \qquad (1)$$

The potential for interaction between charged spacecraft is then limited to regimes in which the separation between vehicles is less than the plasma Debye length. Because the debye length in low-Earth orbit is on the order of centimeters, Coulomb interaction will be negligible. Analysis in this study will be limited to GEO to take advantage of the wealth of plasmaphysical data available for GEO conditions.

An excellent discussion of the space plasma environment can be found in the textbook by Hastings and Garret,[13] some of which is repeated here for convenience. A spacecraft at GEO is at the edge of plasmapause. This collisionless plasma does not follow a single Maxwellian distribution. Instead, plasma parameters must be measured experimentally. The particle detectors on the ATS[14–16] and SCATHA[17] spacecraft have measured plasma variations between 5–10 and 50–80 eV, respectively, for 50 complete days at 1–10-min resolution from 1969 through 1980, bracketing one solar cycle.

Garrett and Deforest[14] fitted an analytical two-temperature model to data collected over 10 different days from ATS-5 spacecraft between 1969 and 1972. These data were selected in such a way as to show a wide range of geomagnetic activity, including plasma injection events, that is, sudden appearance of dense, relatively high-energy plasma at GEO occurring at local midnight. The model gives reasonable and consistent representation of the variations following a substorm injection event at GEO. The parameters for this two-temperature model during average GEO conditions are shown in Table 1, with worst-case GEO conditions given in Table 2.

Table 1 Two-temperature model of average GEO environment[14]

Parameter	Electrons	Ions
n_1, m^{-3}	0.78×10^6	0.19×10^6
kT_1/e, eV	550	800
n_2, m^{-3}	0.31×10^6	0.39×10^6
kT_2/e, eV	8.68×10^3	15.8×10^3

Table 2 Two-temperature model of worst-case GEO environment[14]

Parameter	Electrons	Ions
n_1, m^{-3}	1×10^6	1.1×10^6
kT_1/e, eV	600	400
n_2, m^{-3}	1.4×10^6	1.7×10^6
kT_2/e, eV	2.51×10^4	2.47×10^4

Calculations based on these parameters show that the Debye length at GEO ranges from about 140 m to greater than 1400 m.

B. Modeling Spacecraft Charging

Spacecraft charging, especially differential charging, has been of prime concern to spacecraft designers because of its detrimental effects such as electrostatic discharge in spacecraft and spacecraft subsystems. Reference 18 is one of the tools available to model the plasma environment and spacecraft charging. The space environment effects (SEE) tool allows specification of plasma parameters, spacecraft size, materials, and charging time, whereupon the program predicts potentials of elements on the spacecraft surface. The transient response of a spacecraft in plasma is calculated by modeling the spacecraft–ambient plasma system as an equivalent electric circuit. The equilibrium charge of a vehicle is obtained from the SEE model as the transient solution reaches steady state.

The SEE code was used to predict spacecraft charging, with the intent of using the results of the SEE predictions to calculate Coulomb perturbations. The default spacecraft materials of the SEE code were used for these tests, which are shown in Fig. 1. (See also Table 3.) The SEE code has three preloaded GEO plasma environments, namely worst-case environment, ATS-6 environment, and 4 Sept. 97 environment. (Note that the single-temperature worst-case environment model of the SEE code is different than the two-temperature model of Garrett and Deforest[14] shown in Table 2.) The specifications of these environments are given in Table 4. A representative solution from the SEE tool is shown in Fig. 2. Figure 2 shows an indication of the surface potential distribution on various components of the spacecraft.

C. Natural Forces and Torques

The output of the SEE model includes a value of potential for each finite element of the spacecraft surface. By the use of a vacuum

Table 3 Representative materials and sizes of components in Fig. 1

Component	Size	Material
Chassis	$1 \times 1 \times 1$ m	Kapton®/OSR
Solar arrays	1×4 m	Solar cells BlackKapton
Antennae	1-m diameter	Kapton
Omniantenna	0.2-m diameter 1 m long	Kapton

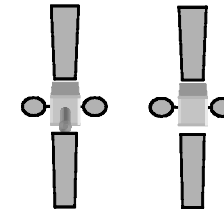

Fig. 1 Spacecraft model used in SEE code seen a) from sun direction and b) from opposite direction.

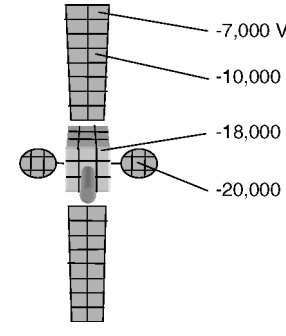

Fig. 2 Representative SEE predictions of spacecraft surface potentials for vehicle subject to worst-case GEO plasma environment in noneclipse conditions.

Green's function,

$$4\pi\varepsilon_0 v_i = \sum_j \frac{q_j}{r_{ij}} \tag{2}$$

it is possible to calculate the equivalent point charge at the center of each finite element that is self-consistent with the potential distribution. The interaction between two charged spacecraft can then be modeled as a superposition of the interactions of the equivalent point charges. For example, the collection of charges on spacecraft B will produce an electric field at a point i on spacecraft A, according to

$$\boldsymbol{E}_i = \frac{1}{4\pi\varepsilon_0}\sum_{j=1}^{nB}\frac{q_j \boldsymbol{r}_{ij}\exp(-|\boldsymbol{r}_{ij}|/\lambda_d)}{|\boldsymbol{r}_{ij}|^3} \tag{3}$$

An electric charge q_i at i will experience a force $\boldsymbol{F}_i = q_i\boldsymbol{E}_i$. The net force on spacecraft A resulting from the n_B charges on spacecraft B is then simply

$$\boldsymbol{F}_{AB} = \sum_{i=1}^{n_A}\boldsymbol{F}_i \tag{4}$$

By the use of the same equivalent point charge method, it is also straightforward to compute the moment on the charged spacecraft A about its geometric center, resulting from the distribution of charges on spacecraft B.

The Coulomb interaction between closely spaced satellites was performed with the SEE code to predict the charging of representative spacecraft. Two identical vehicles, with material properties and physical dimensions as shown in Table 3, were assumed to be in GEO, separated along the direction of orbital velocity to mimic a leader–follower type of formation. The relative orientation of the vehicles is indicated in Fig. 3.

Three GEO plasma environments (Table 4) were used to predict the spacecraft charging in both eclipse and noneclipse conditions due to natural plasma interaction. The forces and torques were computed based on the SEE results for a range of spacecraft separations from 10 to 100 m. The resulting interspacecraft forces and torques about geometric center are shown in Fig. 4. The Coulomb interaction forces were found to be as large as 1 mN for spacecraft 10 m apart in the ATS-6 eclipse environment, with all environments except the 4 Sept. 97 case showing interaction forces greater than 10 μN at the closest spacing. The decay in force with separation is not purely $1/r^2$ due to the finite size effects of the vehicles. At the largest spacing considered (100 m) the inter-spacecraft forces vary from 10^{-10} N up to about 100 nN, depending on the orbital

Table 4 Parameters of the three preloaded GEO plasma environments[18]

Parameter	Worst-case	ATS-6	4 Sept. 97
n_e, m^{-3}	1.2×10^6	1.22×10^6	3.00×10^5
T_e, eV	1.2×10^3	1.6×10^6	0.4×10^3
n_i, m^{-3}	2.36×10^5	2.36×10^5	0.30×10^5
T_{ion}, eV	2.95×10^3	2.95×10^3	0.40×10^3

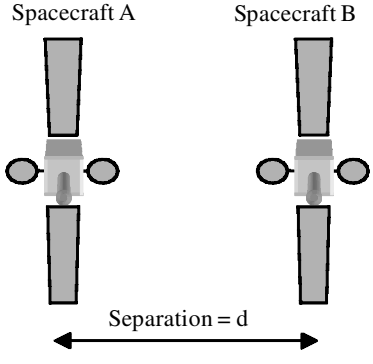

Fig. 3 Relative orientation of two-spacecraft leader–follower formation for natural coulomb interaction study. The vehicles are displaced only along the orbital velocity direction.

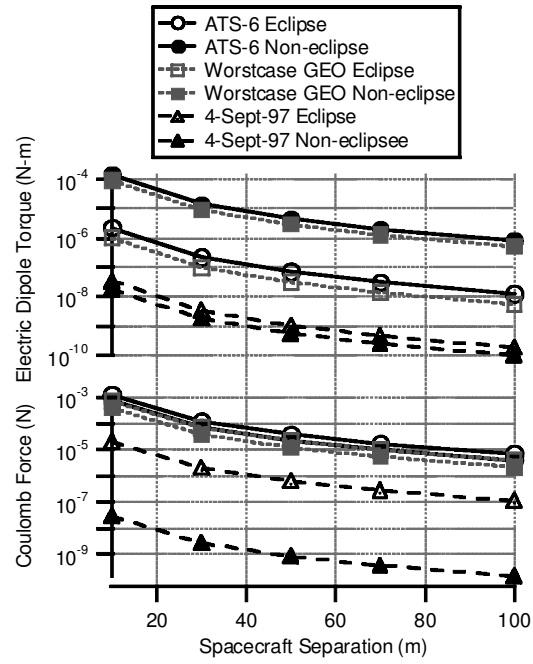

Fig. 4 Predicted interspacecraft coulomb force for two identical satellites in a GEO leader–follower formation as a function of the formation spacing.

conditions used in the SEE prediction. The electric-dipole-induced torques were found to be as large as 100 μN · m for the closest spacing in the ATS-6 eclipse conditions, falling as low as 10^{-10} N · m for the 4 Sept. 97 case at 100-m spacing. The forces and torques arising from natural charging represent undesired perturbations that would be detrimental to a thruster-controlled formation-keeping system.

A surprising result of the Coulomb interaction study was that the magnitude of the interspacecraft forces is comparable with, and may exceed that of, candidate micropropulsion systems proposed for formation keeping. One method for eliminating the parasitic Coulomb forces and torques would be to control the spacecraft charge actively and ensure that vehicle potential remains very near the ambient plasma potential. This could be performed using a hollow-cathode plasma contactor as used on the International Space Station. Another interesting concept, however, is to use an ion or electron emitter to control the spacecraft charge actively and, thus, to regulate the Coulomb force to affect relative propulsion within a formation. The feasibility of forming Coulomb-stabilized formations will be the focus of Sec. III.

III. Formation Dynamics

This section presents a summary of Coulomb formation dynamics that can be found in much more detail in the References.[2] Analytic methods are presented for determining static (rigid) formations of spacecraft, flying in close proximity, using intervehicle Coulomb forces to offset orbital perturbations. The vehicles are approximated as spheres, and it is assumed that the plasma Debye length is much longer than a typical intervehicle separation. Such conditions are a reasonable approximation of formations in GEO with vehicle spacing on the order of tens of meters.

A. Dynamic Equations

As in many formation studies, Hill's equations are used here to describe the motion of spacecraft in a formation relative to a reference point that is assumed to maintain a circular Keplerian orbit. With an application slanted toward separated spacecraft interferometry, the central reference vehicle is referred to as a "combiner" denoted by a 0 subscript, where the surrounding vehicles are called "collectors" denoted by subscripts of 1 through n. It is assumed that the combiner has its own station-keeping system, but that the collectors do not. Thus, the only external forces on the collectors are the Coulomb interactions between them and the combiner.

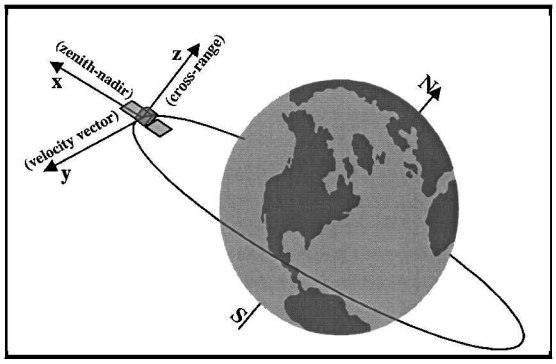

Fig. 5 Illustration of combiner-fixed relative coordinate system used in the Hill's equation formulation (reprinted from Ref. 19).

Within the Hill's system, the motion of the ith collector with respect to the central combiner-fixed coordinate system can be written for a formation of n vehicles interacting via Coulomb forces as

$$\ddot{x}_i - 2\Omega\dot{y}_i - 3\Omega^2 x_i = \frac{\kappa_c}{m_i}\sum_{j=0}^{n}\frac{(x_i - x_j)}{|\boldsymbol{p}_i - \boldsymbol{p}_j|^3}Q_i Q_j, \quad i = 1, \ldots, n \quad \text{and} \quad i \neq j \quad (5a)$$

$$\ddot{y}_i + 2\Omega\dot{x}_i = \frac{\kappa_c}{m_i}\sum_{j=0}^{n}\frac{(y_i - y_j)}{|\boldsymbol{p}_i - \boldsymbol{p}_j|^3}Q_i Q_j, \quad i = 1, \ldots, n \quad \text{and} \quad i \neq j \quad (5b)$$

$$\ddot{z}_i + \Omega^2 z_i = \frac{\kappa_c}{m_i}\sum_{j=0}^{n}\frac{(z_i - z_j)}{|\boldsymbol{p}_i - \boldsymbol{p}_j|^3}Q_i Q_j, \quad i = 1, \ldots, n \quad \text{and} \quad i \neq j \quad (5c)$$

where $\kappa_c = 1/4\pi\varepsilon_0$. The coordinate notation is such that the y direction is along the orbital velocity vector, x is in the zenith–nadir direction, and z is normal to the orbit plane. The axis system is shown in Fig. 5 (see Ref. 19). The interesting difference between this set of equations and the typical Hill's system used in formation studies lies in their coupling: The dynamics of any vehicle in the formation is influenced simultaneously by all of the other vehicles in the group.

A static (rigid) formation geometry must satisfy the Hill's system of equations (5) with zero relative velocity and acceleration for each vehicle ($\dot{x} = \ddot{x} = \dot{y} = \ddot{y} = \dot{z} = \ddot{z} = 0$). The nature of the Coulomb coupling of the system stipulates that control forces can only be applied along the lines connecting spacecraft coordinates. Thus, the goal is to find suitable formation geometries such that the vector sum of the Coulomb forces is sufficient to enable solution of the Hill's system with velocities and accelerations set to zero. The equilibrium system of equations is then found to be

$$-3\Omega^2 x_i = \frac{\kappa_c}{m_i}\sum_{j=0}^{n}\frac{(x_i - x_j)}{|\boldsymbol{p}_i - \boldsymbol{p}_j|^3}Q_i Q_j, \quad i = 1, \ldots, n \quad \text{and} \quad i \neq j \quad (6a)$$

$$0 = \frac{\kappa_c}{m_i}\sum_{j=0}^{n}\frac{(y_i - y_j)}{|\boldsymbol{p}_i - \boldsymbol{p}_j|^3}Q_i Q_j, \quad i = 1, \ldots, n \quad \text{and} \quad i \neq j \quad (6b)$$

$$\Omega^2 z_i = \frac{\kappa_c}{m_i}\sum_{j=0}^{n}\frac{(z_i - z_j)}{|\boldsymbol{p}_i - \boldsymbol{p}_j|^3}Q_i Q_j, \quad i = 1, \ldots, n \quad \text{and} \quad i \neq j \quad (6c)$$

B. Formation Geometries

The method chosen for exploring the behavior of Eqs. (6) was to assume geometric formations and search for solution sets. Although numerous formations were studied in the Reference work,[20] the discussion here will be limited to three canonical cases. The first case considered was a simple linear three-vehicle formation with vehicles separated by L. With the combiner fixed to the origin, three subformations follow, depending on orientation with the axis system. The linear formations are shown in Fig. 6.

The second formation studied was a simple two-dimensional formation that suggests an application for Earth observation through separated spacecraft interferometry. This configuration is shown in Fig. 7, where the four collectors are distributed evenly about the Hill's y and z axes to create a five-spacecraft planar formation. The third formation represented a three-dimensional configuration, with six collectors distributed evenly about the principal axes with spacing L. The three-dimensional formation is shown in Fig. 8.

C. Equilibrium Formation Solutions

Although results will be presented for all of the formations just outlined, the analytic solution method will be presented only for the representative three-spacecraft x-axis aligned case, which we call the Coulomb tether due to its similarity to physical tether configurations. For three spacecraft aligned along the combiner coordinate frame's x axis, as shown in Fig. 6, $n = 3$ and the following relative

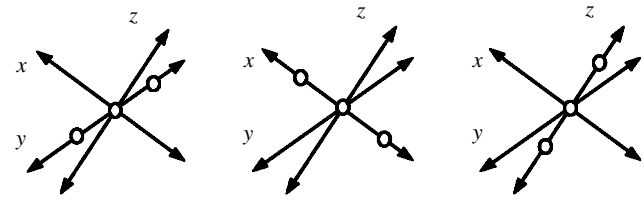

Fig. 6 Linear three-spacecraft formations.

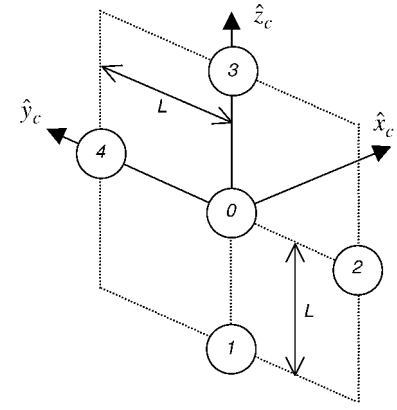

Fig. 7 Illustration of the five-satellite formation.

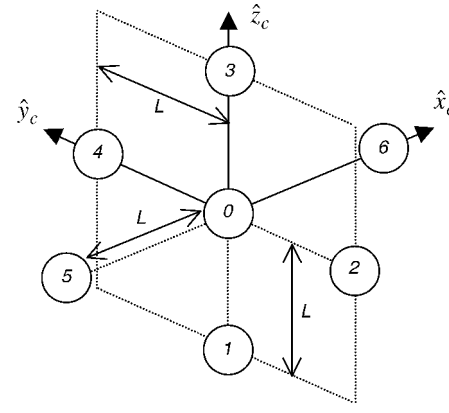

Fig. 8 Illustration of seven-satellite formation.

displacement constraints hold

$$x_1 = L \tag{7a}$$

$$x_2 = -L \tag{7b}$$

$$y_1 = y_2 = z_1 = z_2 = 0 \tag{7c}$$

Formation of all six of the equilibrium equations from Eqs. (6) and elimination of duplicate equations leaves only two conditions:

$$\left(\kappa_c Q_1 Q_2 / 4L^2\right) + \left(\kappa_c Q_1 Q_0 / L^2\right) + 3m_1 L\Omega^2 = 0 \tag{8}$$

$$\left(\kappa_c Q_1 Q_2 / 4L^2\right) + \left(\kappa_c Q_2 Q_0 / L^2\right) + 3m_2 L\Omega^2 = 0 \tag{9}$$

If we further assume that the collectors have equal mass, $m = m_1 = m_2$, and introduce the normalized charges defined by

$$Q_{in} \equiv Q_i / \sqrt{mL^3} \tag{10}$$

then Eqs. (8) and (9) may be written without explicit mass and length dependencies,

$$\kappa_c Q_{1n} Q_{2n}/4 + \kappa_c Q_{1n} Q_{0n} + 3\Omega^2 = 0 \tag{11a}$$

$$\kappa_c Q_{1n} Q_{2n}/4 + \kappa_c Q_{2n} Q_{0n} + 3\Omega^2 = 0 \tag{11b}$$

The subscript n denotes a normalized quantity. Assuming spherical spacecraft, we can use Gauss's law to relate the vehicle surface potential in volts to the equivalent encircled point charge Q_i as $V_i = Q_i / 4\pi\varepsilon_0 r_i$. In a loosely analogous fashion, we will define a normalized voltage V_{in} based on the normalized charge Q_{in}

$$V_{in} \equiv \kappa_c Q_{in} \tag{12}$$

then the equilibrium equations (11) are

$$V_{1n} V_{2n} + 4V_{1n} V_{0n} + 12\kappa_c \Omega^2 = 0 \tag{13a}$$

$$V_{1n} V_{2n} + 4V_{2n} V_{0n} + 12\kappa_c \Omega^2 = 0 \tag{13b}$$

These are readily solved analytically. Given a suitable combiner spacecraft normalized voltage V_{0n}, the two collector normalized voltages must be equal and are

$$V_{1n} = V_{2n} = -2V_{0n} \pm 2\sqrt{V_{0n}^2 - 3\kappa_c \Omega^2} \tag{14}$$

where the combiner normalized voltage must satisfy the constraint

$$V_{0n}^2 - 3k_c \Omega^2 \geq 0 \tag{15}$$

When the actual collector mass m, radius r, separation L, and the orbital angular rate Ω are known, the equilibrium collector physical voltage can be obtained from Eq. (14), and the normalization relationship

$$V_{in} = V_i r_i / \sqrt{mL^3} \tag{16}$$

where the quantity $V_i r_i$ (which is equal to $q_i / 4\pi\varepsilon_0$ by Gauss's law) is called the reduced charge of spacecraft i. The normalized collector voltages, obtained from Eq. (14), are shown in Fig. 9 as a function of the combiner voltage V_{0n}. The angular rate Ω is for a geosynchronous orbit, $\Omega = 7.2915 \times 10^{-5}$ rad/s. Similar analytic methods were used to compute the y- and z-axis aligned formations. These solutions are also shown in Fig. 9.

The three-spacecraft solution set yields some interesting insight. The most trivial case is the y-axis geometry. For this alignment within the Hill's system, a solution set is possible where all of the vehicles are uncharged. Indeed, if any vehicle has a nonzero charge, the net effect of the solution is to cancel the effect of this charge exactly, such that the net force is always zero. The z-axis formation permits solutions where the central combiner has no charge. However, there is no solution where all vehicles are neutral, and

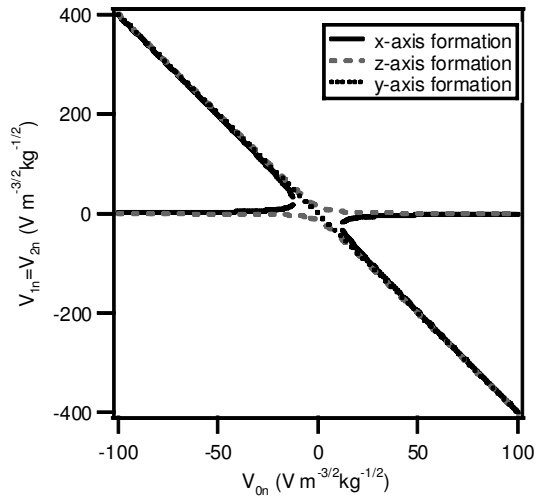

Fig. 9 Analytic solution set for equilibrium three-spacecraft linear formations.

Coulomb forces are required to maintain the static equilibrium. Last, the x-axis formation does not permit any solutions with uncharged spacecraft. There is a clear minimum magnitude for V_{0n} (about 20 in the normalized units), below which no solution is possible.

The analytic method was extended to the five-spacecraft two-dimensional formation and the seven-spacecraft three-dimensional formation. When the constraints of the two- and three-dimensional formations were applied to the equilibrium requirements of Eq. (6), the result was, respectively, 8 and 18 unique necessary conditions for equilibrium.

The two-dimensional five-spacecraft formation yielded two families of solutions. The first family was somewhat trivial and produced solutions where two of the vehicles had zero charge, such that the remaining vehicles assumed the same three-spacecraft linear solutions just described. The second family of solutions was found by forcing the symmetry condition that $Q_1 = Q_3$ and $Q_2 = Q_4$; this reduced the set of eight unique conditions to two:

$$4V_{0n} V_{3n} + V_{3n}^2 + 2\sqrt{2} V_{3n} V_{4n} - \kappa_c \Omega^2 = 0 \tag{17a}$$

$$4V_{0n} V_{4n} + V_{4n}^2 + 2\sqrt{2} V_{3n} V_{4n} = 0 \tag{17b}$$

Equations (17) can be solved conditionally such that Q_1 (and, hence, Q_3) have the form $Q_1 = Q_1(Q_4)$ and $Q_0 = Q_0(Q_1, Q4)$. The resulting solution set is shown in Fig. 10. The solid and dashed lines represent consistent solutions within the set. For example, if $V_{2n} = V_{4n} = -50$, then either $V_{1n} = V_{3n} = -10$ with $V_{0n} = 20$, or $V_{1n} = V_{3n} = -50$ with $V_{0n} = 50$.

The seven-spacecraft equilibrium solution was found when the symmetry condition $Q_1 = Q_3$, $Q_2 = Q_4$, and $Q_5 = Q_6$, was required, which reduced the set of 18 conditions to three unique equations:

$$\left(\kappa_c / L^2\right) Q_0 Q_1 + \left(\sqrt{2}/2L^2\right)\kappa_c Q_1 Q_2 + \kappa_c Q_1^2 / 4L^2 + \left(\sqrt{2}/2L^2\right)\kappa_c Q_1 Q_5 - mL\Omega^2 = 0 \tag{18a}$$

$$(1/L^2) k_c Q_0 Q_2 + \left(\sqrt{2}/2L^2\right)\kappa_c Q_1 Q_2 + (1/4L^2)\kappa_c Q_2^2 + \left(\sqrt{2}/2L^2\right)\kappa_c Q_2 Q_5 = 0 \tag{18b}$$

$$\left(\kappa_c Q_0 Q_5 / L^2\right) + \left(\sqrt{2}/2L^2\right)\kappa_c Q_2 Q_5 + \left(\sqrt{2}/2L^2\right)\kappa_c Q_1 Q_5 + \kappa_c q_5^2 / 4L^2 + 3mL\Omega^2 = 0 \tag{18c}$$

Given a value of Q_2 (or, similarly, Q_4), Eq. (18) can be solved analytically such that the collectors' charges are functions of Q_2

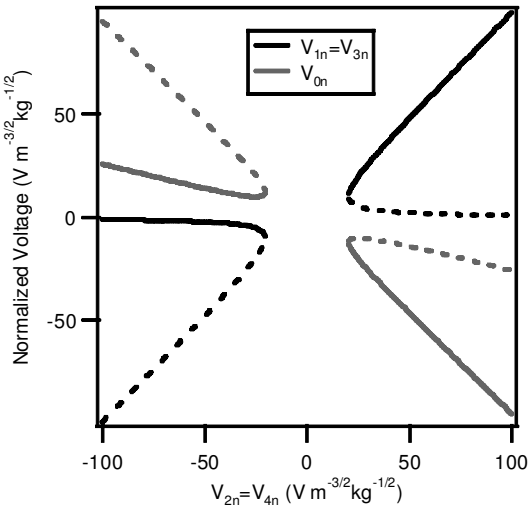

Fig. 10 Solution set for equilibrium five-spacecraft two-dimensional formation.

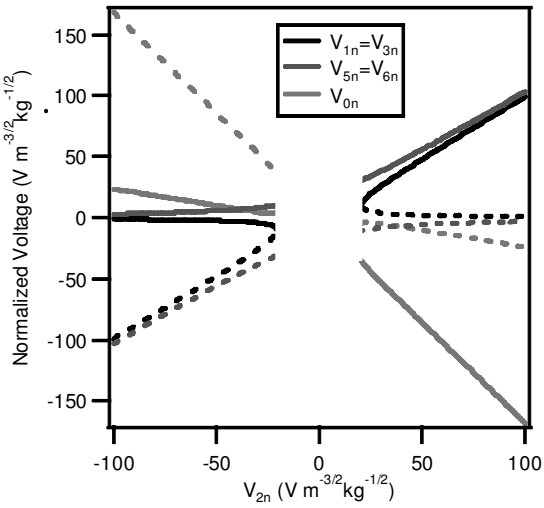

Fig. 11 Equilibrium solution set for seven-spacecraft three-dimensional formation.

$$Q_1 = Q_3 = Q_1(Q_2) \tag{19a}$$

$$Q_5 = Q_6 = Q_5(Q_2) \tag{19b}$$

The combiner charge Q_0 can then be expressed as $Q_0 = Q_0(Q_1, Q_2, Q_5)$. A plot of the equilibrium solution set is shown in Fig. 11. In Fig. 11, solid and dashed lines represent consistent solutions within the set. For example, if V_{2n} is –50, then the solution is either $V_{1n} = V_{3n} = -50$, $V_{5n} = V_{6n} = -60$, with $V_{0n} = 75$ or $V_{1n} = V_{3n} = -10$, $V_{5n} = V_{6n} = 8$, with $V_{0n} = 10$.

D. Physical Estimates

The normalized and reduced variables utilized in the analytic solution method can be used to estimate physically meaningful parameters. It is apparent from a study of Figs. 9–11 that an infinite number of possible vehicle charge states (voltages) exist for any of the formations. One method of selecting an optimal set of parameters was based on minimization of the overall charging required by the formation. By the use of the sum of the squares of the vehicle charges as a cost function, the optimum solution for each formation was calculated analytically. The optimal solutions can be used to provide estimates of physical parameters. For discussion's sake, it is assumed here that the vehicles each have identical mass of 150 kg and that the interspacecraft separation for all of the formations was $L = 10$ m. From the optimum solutions, the value of reduced charge $V_i r_i$ can be calculated. The reduced charge can be thought of as the surface potential required for a spherical vehicle with 1-m radius, with scaling to different radii vehicles as a straightforward calculation. The magnitude of optimal vehicle reduced charge for each formation is presented in Table 5.

Table 5 Minimum total charge[a] equilibrium solutions for each of the formations[b]

Formation	V_0r_0	V_1r_1	V_2r_2	V_3r_3	V_4r_4	V_5r_5
Three x axis	13.8	13.8	13.8	——	——	——
Three z axis	2.39	2.39	2.39	——	——	——
Five	4.78	3.96	7.92	3.96	7.92	——
Seven	12.7	3.96	7.92	3.96	7.92	11.2

[a]The units of the vehicle-reduced charges $V_i r_i$ are in kilovolt meters. The numbers can be thought of as the surface potential of a 1-m-rad spherical spacecraft in kilovolts.
[b]For the linear formations, only the x-axis aligned and z-axis aligned three-spacecraft solutions are shown.

IV. Propulsion Figures of Merit

The purpose of this section is to evaluate some fundamental performance metrics of a coulomb control system on a spacecraft formation. Aspects such as control force, input power, required consumable mass, and environment interaction will be calculated for a simple two-spacecraft system.

A. Required Power

An isolated spacecraft will assume equilibrium potential (voltage) such that the net environmental current due to plasma and photoelectron emission is zero. It is possible to change the vehicle potential by emitting a charge from the spacecraft. For example, if it is desired to drive the spacecraft potential lower than equilibrium (more negative), the emission of positive ions from the vehicle will cause a net surplus of onboard electrons and a lowering of the potential. To emit such a current, the charges must be ejected from the vehicle with sufficient kinetic energy to escape the spacecraft potential well. Thus, if the vehicle is at a (negative) potential $-V_{SC}$, then ions must be emitted from a source operating at a power supply voltage V_{PS} greater than $|-V_{SC}|$.

Basic concepts can be used to calculate the power required to maintain the spacecraft at some steady-state potential. To maintain the spacecraft at a voltage of $|V_{SC}|$, current must be emitted in the amount of $|I_e| = 4\pi r^2 |J_p|$, where J_p is the current density to the vehicle from the plasma, using a power supply having a voltage of at least $|V_{PS} = V_{SC}|$. Quantitatively,

$$P = |V_{SC} I_e| \tag{20}$$

For a two-spacecraft formation with each vehicle using power P, the total system power is just the sum of the individual power to each vehicle. Under the assumption of a spherical spacecraft and by the use of Gauss's law to relate the surface potential to the encircled point charge, it is possible to relate the Coulomb force (thrust) on a vehicle to the emission current and the required power

$$F_C = 4\pi\varepsilon_0 e^{-d/\lambda_d} \frac{r_A r_B P^2}{d^2 I_{eA} I_{eB}} \tag{21}$$

Equation (21) yields the power required to produce a steady-state thrust for a given emission current. Because the space environment will be constantly changing (and, hence, the emission current to maintain steady-state), it is important to calculate the required power to affect a change in potential from some initial value to a desired steady-state value. In the pedagogical analysis here, the capacitance of the spherical spacecraft can be used to estimate the power required for a change in voltage (thrust). With an equivalent circuit model where $dV_{SC}/dt = I/C$, the rate of change of spacecraft potential can be related to the current absorbed from the plasma and the emitted control current:

$$\frac{dV_{SC}}{dt} = \frac{4\pi r^2 J_p + I_e}{4\pi\varepsilon_0 r} \tag{22}$$

The value of J_p can easily be evaluated with traditional plasma probe theory for a sphere and will take the form

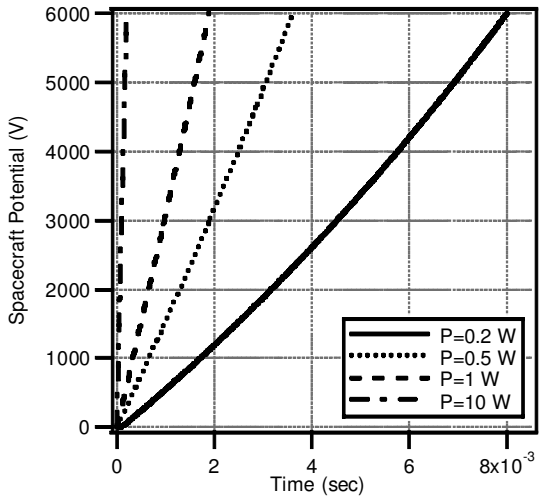

Fig. 12 Numerical integration of the transient response of a 1-m-diam model spacecraft in an average GEO plasma as a function of the power in the emitted control beam.

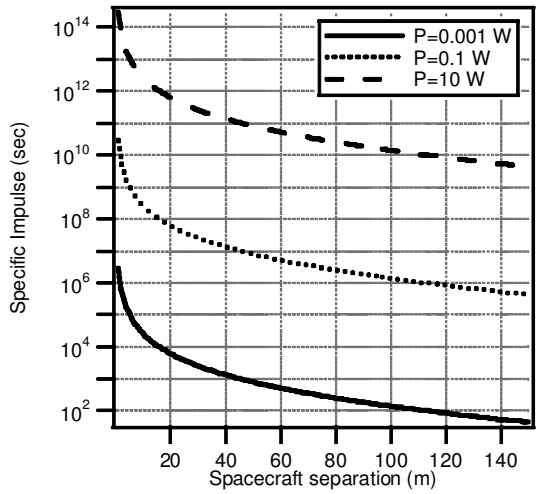

Fig. 13 Specific impulse for a two-spacecraft coulomb formation as a function of spacecraft separation d and input power P.

$J_p = J_p(V_{SC}, n_e, n_i, T_e, T_{ion})$. If V_{final} is the desired steady-state spacecraft voltage, then the emission current power supply must have power $P = I_e V_{final}$. By substitution of $I_e = P/V_{final}$ into Eq. (22) and the analytic expression for J_p from probe theory for the plasma current, an explicit equation is obtained of the form

$$\frac{dV_{SC}}{dt} = f(P, V_{SC}, n_e, n_i, T_e, T_{ion}, r) \tag{23}$$

which can be numerically integrated to produce a function

$$V_{SC} = V_{SC}(n_e, n_i, T_e, T_i, r, P, t) \tag{24}$$

As a numerical example, Fig. 12 shows a plot of the function obtained for Eq. (24) assuming a 1-m-diam spacecraft charging from $V_{SC} = 0$ to $V_{final} = 6$ kV in the average GEO plasma environment. From Fig. 12, it is evident that only 200 mW of power is required to change the spacecraft potential by 6 kV within 8 ms.

B. Mass Flow Rate and I_{sp}

Mass flow rate is defined by the rate of gaseous ions expelled per unit of time to maintain the potential of the vehicle. Because electrons have negligible mass, we can say that the mass flow rate of electrons is negligible and, thus, driving the potential positive requires zero mass flow. If I_e is the emission current constituting ions and m_{ion} is the mass of ion, then the mass flow rate is given by

$$\dot{m} = I_e m_{ion}/q_{ion} \tag{25}$$

Because the only purpose of the ion emission is to carry charge (and not momentum) from the vehicle, it makes sense to use the least massive ions that are practical. For a two-spacecraft combination, propellant mass flow rate will be the sum of mass flow rates for individual spacecraft and can be related to their individual emission currents

$$\dot{m}_{total} = (m_{ion}/q_{ion})(I_{ea} + I_{eB}) \tag{26}$$

A common performance parameter used for propulsion systems is specific impulse I_{sp}. This parameter compares the thrust derived from a system to the required propellant mass flow rate.[21] Although I_{sp} is traditionally used as a parameter to evaluate momentum transfer (rocket) systems, we can use the formal definition to compare the coulomb system. For a Coulomb control system the specific impulse I_{sp} is given by

$$I_{sp} = F/\dot{m}_{total}\, g_0 \tag{27}$$

Because Coulomb force calculations are meaningless for a single vehicle, we will treat the system as two separate vehicles, each subject to a force of F_c given by Eq. (21), so that the sum of the forces experienced by all spacecraft in the formation is $F = 2F_c$:

$$I_{sp} = \frac{8\pi\varepsilon_0 e^{-d/\lambda_d} q_{ion}}{g_0 m_{ion}} \frac{r_A r_B P^2}{d^2 I_{eA} I_{eB} (I_{eA} + I_{eB})} \tag{28}$$

If $r_A = r_B = r_{sc}$, and $I_e = I_{eA} = I_{eB}$, then Eq. (28) becomes,

$$I_{sp} = \frac{4\pi\varepsilon_0 e^{-d/\lambda_d} q_{ion} r_{SC}^2 P^2}{g_0 m_{ion} d^2 I_e^3} \tag{29}$$

Note that, unlike a rocket system, the definition of I_{sp} of a Coulomb system is meaningless for a single vehicle. For a formation of two spacecraft, Eq. (29) indicates that the specific impulse of the formation is a function of the radii of the spacecraft, power supplied to the ion (electron) gun, the separation between the two spacecraft, the emission currents of both vehicles, and the mass of the charge carriers m_{ion}.

Consider a two-spacecraft formation with identical 1-m-diam vehicles in the average GEO plasma environment, charged to the same negative potential. To reach and maintain this negative potential, the vehicles must emit an ion current. Consequently, the spacecraft will attract ion saturation current from the plasma. Hence, I_e must be equal to the plasma ion saturation current for steady state. It is apparent that light ions will provide the most efficient I_{sp}, and so assume that the emitted species is H^+. Calculated values of specific impulse for each vehicle in the formation are shown in Fig. 13 for various system input power levels. For 1-mW systems with vehicle separation on the order of 20 m, I_{sp} values of 10^4 s are obtained, with values increasing to 10^{10} s for just 1 W of power. Note that, for a positive vehicle potential, the emitted species would be electrons and, thus, the calculated values of I_{sp} would be a factor of 2000 greater.

C. Emission Current Jet Force

Generating a net charge on a spacecraft for coulomb force requires the emission of a current. Because the charge is carried away from the vehicle by particles with non-zero mass, such mass ejection results in a momentum jet force on the vehicle, as in a traditional electric propulsion thruster. In the case of electron emission, the mass of the charge carriers is insignificant, and the resulting jet force is negligible. Ion emission, however, may produce a significant reaction force. It is instructive to consider how the Coulomb force between spacecraft compares with the momentum reaction on the vehicle induced by the beam of ion current. The reactive thrust force of an ejected mass flow is computed as

$$F_J = \dot{m} u_e \tag{30}$$

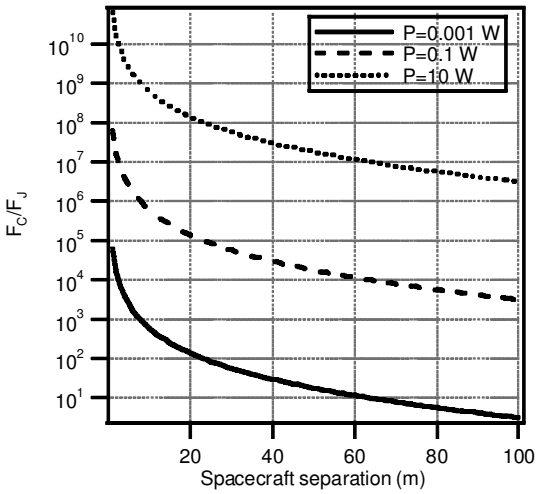

Fig. 14 Comparison between induced coulomb force and the momentum reaction of the emitted ion beam used to maintain the spacecraft charge for three power levels.

Given steady-state Coulomb force generation, the ions will be electrostatically accelerated through a spacecraft potential of V_{SC}, such that

$$u_e = \sqrt{2q_{\text{ion}}V_{SC}/m_{\text{ion}}} \tag{31}$$

With this simplification, and recognition that the mass flow is related to the emission current, the momentum jet force of the emitted ion current is

$$F_J = I_e\sqrt{2m_{\text{ion}}V_{SC}/q_{\text{ion}}} \tag{32}$$

The jet force can also be written in terms of the input power to the emission system as

$$F_J = \sqrt{2m_{\text{ion}}PI_e/q_{\text{ion}}} \tag{33}$$

We can compare the magnitude of the jet reaction force with the induced Coulomb force between two vehicles. Assume identical spacecraft charged to the same value of V_{SC}. From Eqs. (21) and (33), we can write the ratio of F_C/F_J (taking F_C as the total Coulomb force on both vehicles) in terms of the input power as

$$\frac{F_C}{F_J} = 4\sqrt{2}\pi\varepsilon_0\sqrt{\frac{q_{\text{ion}}}{m_{\text{ion}}}}\frac{r_A r_B P^{\frac{3}{2}}e^{-d/\lambda_d}}{I_{eA}I_{eB}(I_{eA}+I_{eB})^2} \tag{34}$$

If $r_A = r_B = r_{SC}$, and $I_e = I_{eA} = I_{eB}$, then Eq. (34) becomes

$$\frac{F_C}{F_J} = 2\sqrt{2}\pi\varepsilon_0\sqrt{\frac{q_{\text{ion}}}{m_{\text{ion}}}}\frac{r_{SC}^2 P^{\frac{3}{2}}e^{-d/\lambda_d}}{I_e^3 d^2} \tag{35}$$

For a formation of two spacecraft, we find that the F_C/F_J ratio is a function of the radii of the spacecraft, power supplied to the ion (electron) gun, the separation between the two spacecraft, and the emission currents. Similar to the calculations for specific impulse, if we consider formation of two identical spacecraft in GEO having the same diameter of 1 m, charged to same high negative voltage V_{SC}, and using the same power P, they will each draw ion saturation current from the ambient plasma. Hence, the (ion) emission current I_e will be also the same. Fig. 14 shows the ratio of Coulomb to jet force under the assumption of hydrogen ion emission in average GEO plasma.

Note from Fig. 14 that, for separations up to 100 m, and system power greater than 1 mW, the Coulomb force is considerably higher than the jet force. This implies two conclusions: 1) The Coulomb force is a wiser use of power than a mass-emitting electron-propulsion thruster. 2) The directional jet force will not be a significant perturbation to the Coulomb control system.

V. Conclusions

A new mode of potential spacecraft interaction was identified for closely spaced formations of vehicles in high-Earth orbit. By the use of typical GEO conditions found in the literature, modeling and calculations were performed to show that Coulomb forces between vehicles may be as large as 1 mN for spacecraft 10 m apart, with electric dipole disturbance torques as high as 100 μN · m at the closest separations. For larger spacing, most models showed the potential for forces of tens of micro-Newtons and micro-Newton meter torques persisting out to 50-m separation.

The Coulomb disturbance forces are commensurate with those expected from micropropulsion systems that will likely be used for formation maintenance. In an exploratory study, the possibility to exploit the Coulomb interactions purposefully as formation-keeping forces was investigated. The dynamic equations were formed within Hill's relative coordinate system for a collection of interacting vehicles. Analytic methods were developed to prove the existence of static equilibrium solutions that used only Coulomb forces for propulsion within the swarm. Unique solution sets were found for one-dimensional three-spacecraft formations, a two-dimensional five-spacecraft formation, and a three-dimensional seven-spacecraft formation. Assuming 150-kg vehicles with physical dimensions of 1 m, it was shown that kilovolt spacecraft potentials are sufficient to maintain most formations in a rigid geometry.

The Coulomb control system was evaluated in classical propulsion terms. It was shown that the specific impulse can be as high as 10^{13} s. Because of the novel scaling of thrust, power, and specific impulse in this nonmomentum thrust system, power levels as low as tens of milliwatts were shown sufficient to maintain the forces and to change their magnitude within a timescale of milliseconds.

Acknowledgments

Work reported here was supported by the NASA Institute for Advanced Concepts under a Phase I contract. This support is gratefully acknowledged.

References

[1]Pollard, J. E., Chao, C. C., and Janson, S. W., "Populating and Maintaining Cluster Constellations in Low-Earth Orbit," AIAA Paper 99-2878, June 1999.

[2]Walker, J. G., "Geometry of Satellite Clusters," *Journal of British Interplanetary Society*, Vol. 35, No. 8, 1982, pp. 345–354.

[3]Murdoch, J., and Pocha, J. J., "The Orbit Dynamics of Satellite Clusters," International Astronautical Congress, Paper IAF-82-54, Sept.–Oct. 1982.

[4]Chao, C. C., Pollard, J. E., and Janson, S. W., "Dynamics and Control of Cluster Orbits for Distributed Space Missions," American Astronautical Society, Paper AAS-99-126, Feb. 1999.

[5]Kong, E. M. C., Miller, D. W., and Sedwick, R. J., "Exploiting Orbital Dynamics for Aperture Synthesis Using Distributed Satellite Systems: Applications to a Visible Earth Imager System," American Astronautical Society, Paper AAS-99-122, Feb. 1999.

[6]Sedwick, R., Miller, D., and Kong, E., "Mitigation of Differential Perturbations in Clusters of Formation Flying Satellites," American Astronautical Society, Paper AAS-99-124, Feb. 1999.

[7]Micci, M. M., and Ketsdever, A. D., *Micropropulsion for Small Spacecraft*, Progress in Astronautics and Aeronautics, Vol. 187, AIAA, Reston, VA, 2000.

[8]Vassar, R. H., and Sherwood, R. B., "Formation Keeping for a Pair of Satellites in a Circular Orbit," *Journal of Guidance, Control, and Dynamics*, Vol. 8, No. 2, 1985, pp. 235–242.

[9]Jilla, C. D., "Separated Spacecraft Interferometry—System Architecture Design and Optimization," M.S. Thesis, Dept. of Aeronautics and Astronautics, Massachusetts Inst. of Technology, Cambridge, MA, Feb. 1999.

[10]Kong, E. M., "Optimal Trajectories and Orbit Design for Separated Spacecraft Interferometry, M.S. Thesis, Dept. of Aeronautics and Astronautics, Massachusetts Inst. of Technology, Cambridge, MA, Nov. 1998.

[11]Yashko, G., "Ion Micro-Propulsion and Cost Modeling for Satellite Clusters," M.S. Thesis, Dept. of Aeronautics and Astronautics, Massachusetts Inst. of Technology, Cambridge, MA, June 1998.

[12]Hacker, T. L., "Performance of a Space-Based GMTI Radar System Using Separated Spacecraft Interferometry," M.S. Thesis, Dept. of Aeronautics and Astronautics, Massachusetts Inst. of Technology, Cambridge, MA, May 2000.

[13]Hastings, D., and Garret, H., Spacecraft–Environment Interactions, Cambridge Univ. Press, Cambridge, England, U.K., 1996, pp. 44–71.

[14]Garrett, H. B., and Deforest, S. E., "An Analytical Simulation of the Geosynchronous Plasma Environment," *Planetary Space Science*, Vol. 27, No. 8, 1979, pp. 1101–1109.

[15]Garrett, H. B., Schwank, D. C., and Deforest, S. E., "A Statistical Analysis of the Low Energy Geo-Synchronous Plasma Environment—I. Electrons," *Planetary Space Science*, Vol. 29, No. 10, 1981, pp. 1021–1044.

[16]Garrett, H. B., Schwank, D. C., and Deforest, S. E., "A Statistical Analysis of the Low Energy Geo-Synchronous Plasma Environment—II. Protons," *Planetary Space Science*, Vol. 29, No. 10, 1981, pp. 1045–1060.

[17]Mullen, E. G., Gussenhoven, M. S., and Hardy, D. A., "SCATHA Survey of High-Voltage Spacecraft Charging in Sunlight," *Journal of Geophysical Research*, Vol. 91, No. A2, 1986, pp. 1474–1490.

[18]"Interactive Spacecraft Charging Handbook," Maxwell Technologies System Division, Space Environment Effect Program, NASA Marshall Space Flight Center. [code and specifications], URL: http://see.msfc.nasa.gov/ee/model_charging.html [cited 1 April 2003].

[19]Kong, E. M., "Optimal Trajectories and Orbit Design for Separated Spacecraft Interferometry," M.S. Thesis, Dept. of Aeronautics and Astronautics, Massachusetts Inst. of Technology, Cambridge, MA, Nov. 1998.

[20]Chong, J.-H., "Dynamic Behavior of Spacecraft Formation Flying Using Coulomb Forces, M.S. Thesis, Dept. of Mechanical Engineering—Engineering Mechanics, Michigan Technological Univ., Houghton, MI, May 2002.

[21]Humble, R. W., Henry, G. N., and Larson, W. J., *Space Propulsion Analysis and Design*, McGraw–Hill, New York,1995, p. 10.